Cell Reports
Physical Science

CellPress
OPEN ACCESS

Article

An engineered, non-diazotrophic cyanobacterium and its application in bioelectrochemical nitrogen fixation

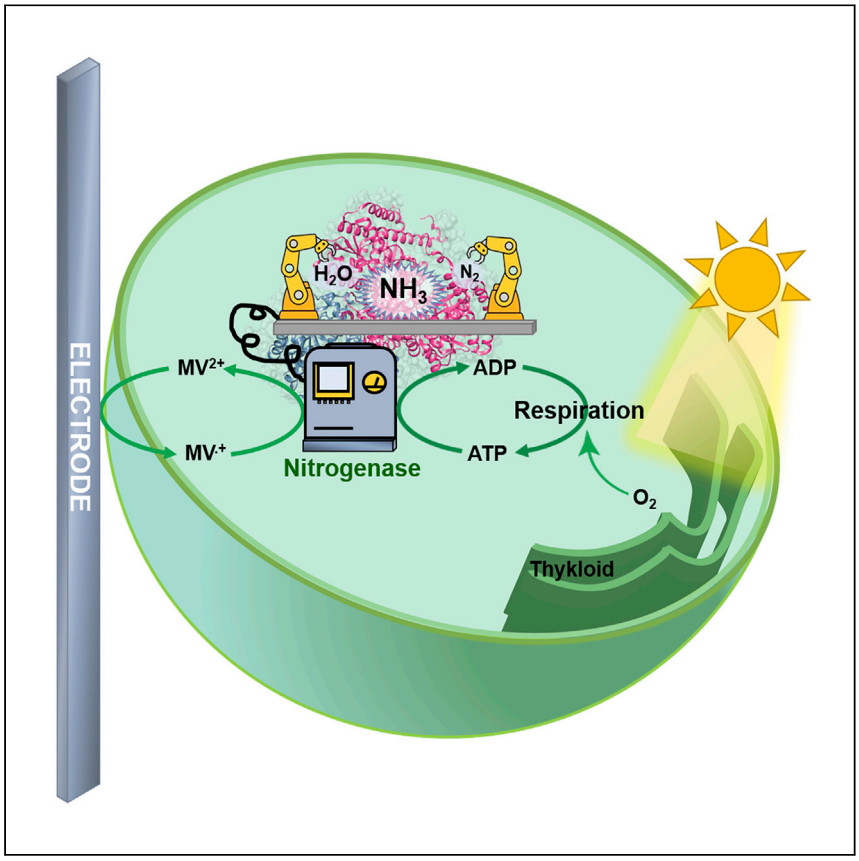

The heterologous expression of nitrogenase in the non-diazotrophic cyanobacterium *Synechococcus elongatus* PCC 7942 is realized for nitrogen fixation by Dong et al. The engineered *S. elongatus* PCC 7942 strain is further employed in an e-BNF system for bioelectrocatalytic ammonia production. Powered by electrical and light energy, microbial N_2 fixation and ammonia generation are achieved.

Fangyuan Dong, Yoo Seok Lee, Erin M. Gaffney, Matteo Grattieri, Helena Haddadin, Shelley D. Minteer, Hui Chen

chen.hui@utah.edu

Highlights

A non-diazotrophic cyanobacterium is engineered for N_2-fixation activity

The addition of DCMU protects the expressed O_2-sensitive intracellular nitrogenase

The e-BNF supplies adequate external electrons and improves the turnover of nitrogenase

The secreted NH_3 generated from the turnover of nitrogenase is successfully quantified

Dong et al., Cell Reports Physical Science *2*, 100444
June 23, 2021
https://doi.org/10.1016/j.xcrp.2021.100444

Cell Reports
Physical Science

CellPress
OPEN ACCESS

Article

An engineered, non-diazotrophic cyanobacterium and its application in bioelectrochemical nitrogen fixation

Fangyuan Dong,[1] Yoo Seok Lee,[1] Erin M. Gaffney,[1] Matteo Grattieri,[1] Helena Haddadin,[1] Shelley D. Minteer,[1] and Hui Chen[1,2,*]

SUMMARY

The reduction of chemically inert nitrogen to ammonia is a critical step in the global nitrogen cycle. Microbial nitrogen fixation is a promising way to realize nitrogen reduction and ammonia production at mild conditions. Here, we report an engineered, non-diazotrophic *Synechococcus elongatus* PCC 7942 strain with nitrogen fixation activity that is constructed by integrating a modified nitrogenase gene cluster into the genome. The engineered *S. elongatus* PCC 7942 strain is employed in a bioelectrochemical nitrogen-fixation (e-BNF) system for ammonia production. Because the e-BNF system supplies adequate external electrons for the turnover of nitrogenase, the nitrogen fixation activity of the engineered *S. elongatus* PCC 7942 strain is significantly improved. After 48 h of reaction, the e-BNF system accumulates 173 μM of NH_3, which is 21 times higher than that generated from solely photosynthesis-driven nitrogen fixation, with faradaic efficiency of 6.85%. This work may provide new insight into biological nitrogen-fixation systems and ammonium production.

INTRODUCTION

Dinitrogen (N_2) is the most ubiquitous atmospheric gas and the ultimate nitrogen source for nitrogenated industrial and natural compounds. The reduction of chemically inert N_2 to more biologically and industrially useful forms of nitrogen, such as ammonia (NH_3), is a critical step in the global nitrogen cycle.[1] Currently, the production of ammonia remains dependent on the Haber-Bosch process that operates at high temperatures (>500°C) and pressures (20 MPa).[2] Because the Haber-Bosch process results in 1% global energy consumption and production of 3% of global CO_2, it has motivated the exploration of alternatives for N_2 activation and fixation, including a rising list of approaches involving plasma induction,[3] metallic complex catalysis,[4–6] and electrocatalysis.[2,7–9] Biologically, nitrogenase is the only enzyme known to reduce N_2 to NH_3 at mild conditions (<40°C, atmospheric pressure) at the expense of a reductant and ATP hydrolysis.[7,10,11] A novel bioelectrocatalytic process based on the purified nitrogenase has been successfully established by the Minteer[2,12–15] group to realize the N_2 reduction and NH_3 production with electron mediators shuttling electrons between the electrode and the nitrogenase. The bioelectrocatalytic method provides a new perspective for N_2 fixation at ambient temperature and pressure and completely eliminates CO_2 emission.

In comparison with using purified nitrogenase, the employment of microbial cells for N_2 fixation is an easier method because the microbial cell provides a stable

[1]Department of Chemistry, University of Utah, 315 South 1400 East, RM 2020, Salt Lake City, UT 84112, USA

[2]Lead contact

*Correspondence: chen.hui@utah.edu

https://doi.org/10.1016/j.xcrp.2021.100444

and self-repairing environment for the nitrogenase and avoids the complicated and time-consuming process of protein purification. In nature, microbial N_2 reduction is limited to a small subset of prokaryotes, named diazotrophs, which have been identified in diverse taxonomic groups.[16] *Anabaena variabilis* is a well-known cyanobacterium that can differentiate heterocysts for nitrogen fixation under the nitrogen-deficient condition.[17] Ammonia is not continuously produced but, rather, regulated by cellular requirements.[17–20] *Xanthobacter autotrophicus*, a diazotrophic bacterium, which is able to simultaneously express hydrogenase and nitrogenase, was also used for sustainable ammonia and biofertilizer production.[21] To further expand the research field of microbial nitrogen fixation via endowing nitrogen-fixation ability to non-diazotrophic species, the heterologous expression of the nitrogenase gene cluster (the *nif* gene cluster) in genetic engineering model microbes has attracted considerable attention. However, transferring the complete N_2 fixation machinery to a heterologous host is not an easy task. The biosynthesis of nitrogenase is a highly intricate process and encompasses all components required for the assembly of a functional dinitrogenase and dinitrogenase reductase. Apart from the structural genes encoding dinitrogenase (*nif*D and *nif*K) and dinitrogenase reductase (*nif*H), many other regulatory *nif* genes are required for the biosynthesis, and insertion of metalloclusters into dinitrogenase and dinitrogenase reductase subunits is also required.[22,23] The total number of genes necessary for a functional nitrogenase differs among organisms and is usually estimated to be 10–20.[24,25] In previous studies, *Escherichia coli*, a non-diazotrophic bacterium with explicit genetic background and mature genetic-engineering-operation methods, has been engineered for nitrogen fixation via the heterologous expression of the *nif* gene cluster from various diazotrophic species.[22,26–29] Cyanobacteria are also of interest for engineering the ability to fix N_2. A successful example of this was demonstrated by introducing the *nif* gene cluster from cyanobacterium *Cyanothece* 51142 into the non-diazotrophic cyanobacterium *Synechocystis* 6803.[30] The *nif* gene cluster has even been introduced directly into the chloroplast genome of the single-cell green alga *Chlamydomonas reinhardtii* to express the dinitrogenase reductase as an active moiety.[31] There have also been attempts to engineer eukaryotic species, such as *Saccharomyces cerevisiae*, to express nitrogenase.[32–36]

Although some breakthroughs in biological N_2 fixation have been achieved, there are still many unsolved problems. For bioelectrochemical N_2 fixation based on purified nitrogenase, the purification of dinitrogenase and dinitrogenase reductase under anaerobic conditions is complicated and time consuming. Moreover, an expensive ATP-regeneration system is required to drive the N_2 fixation.[37] Although some attempts at developing ATP-free systems have been carried out, the efficiency of N_2 fixation and NH_3 production is still low.[38,39] For microbial N_2 fixation, the advantages are that the cumbersome nitrogenase purification process can be avoided, and ATP can be regenerated and recycled via *in vivo* metabolic activities. However, some new issues cannot be ignored either. For natural diazotrophic microorganisms, such as *A. variabilis*, only 10% of the cells can form heterocysts that have the capacity to perform N_2 fixation. Moreover, ammonium is not continuously produced by natural diazotrophic microorganisms but is regulated by cellular requirements.[17–20] For engineered non-diazotrophs, the N_2-fixation activity of recombinant nitrogenase is much lower in comparison with that of the counterpart in native hosts because of the difficulty of coupling the cellular metabolism to supply the reducing power for the N_2-fixation process. The enzymes related to electron transport need to be further introduced into the engineered host cell to enhance electron supply for the turnover of heterologously expressed nitrogenase.[40] In addition, the reduction of every single N_2 molecule consumes eight electrons (Equation 1).[41] The extra electron

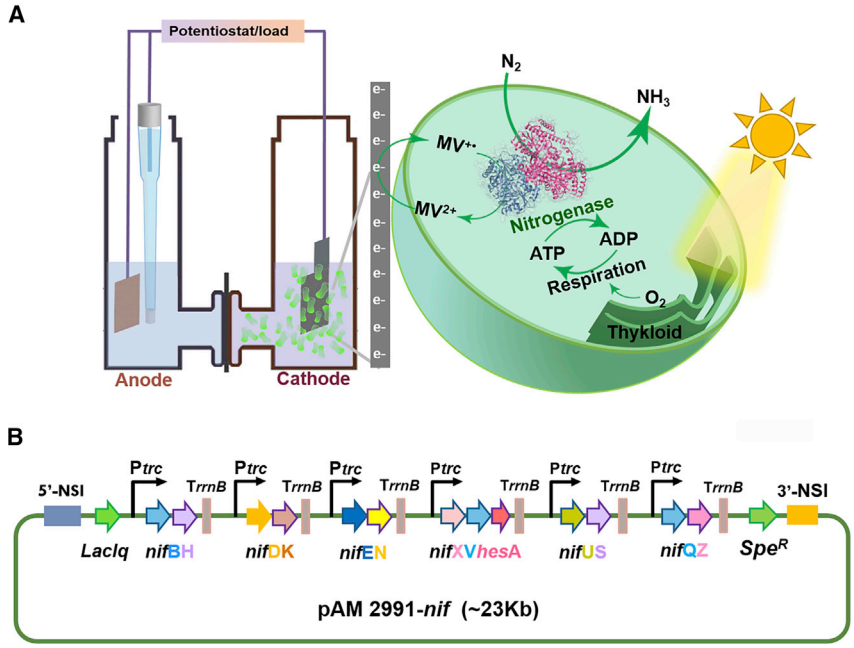

Figure 1. Design of microbial electrolyte cell and *nif* gene cluster for the microbial N_2 fixation based on the engineered *S. elongatus* PCC 7942

(A) The schematic representation of the e-BNF system.

(B) The design and construction of the *nif* gene cluster. P*trc*, trc promoter; T*rrnB*, rrnB terminator; NSI, neutral site 1; *LacIq*, laclq repressor gene; Spe^R, spectinomycin resistance gene.

consumption is a potential problem in disturbing the redox balance inside the cell. The supplementation of external electrons could be a feasible solution to that problem.[42] Cyanobacterial genetic-engineering model microorganisms, such as *Synechococcus elongatus* PCC 7942 and *Synechocystis* sp. PCC 6803, are promising hosts for heterologous *nif* gene cluster expression because they are easy to cultivate, suitable for expressing prokaryotic proteins, and possessing the ability to synthesize metal cofactors. However, the challenge of using cyanobacteria as the recombinant nitrogenase expression host is that the generated O_2 via photosynthesis can deactivate the nitrogenase. So far, only a few successful examples of the heterologous expression of the *nif* gene cluster in photoautotrophs have been achevied.[30,31,43] However, no research has been able to quantify the concentration of secreted extracellular ammonium either because the production of ammonium is so low or the ammonium is not being secreted from the cell.

$$16\ \mathrm{Mg\ ATP} + N_2 + 8e^- + 8H^+ \rightarrow 16\ \mathrm{Mg\ ADP} + 2NH_3 + H_2 + 16\ \mathrm{Pi} \qquad \text{(Equation 1)}$$

In view of the above problems, we establish a bioelectrochemical N_2 fixation (e-BNF) system (Figure 1A) for N_2 fixation based on the use of engineered cyanobacterium *S. elongatus* PCC 7942. In detail, the minimal *nif* gene cluster from *Paenibacillus* sp. WLY78.7[27] is modified (Figure 1B) and transformed into *S. elongatus* PCC 7942 to realize the heterologous expression of nitrogenase. Because *S. elongatus* PCC 7942 is a non-diazotroph, this strain does not possess the feedback regulation mechanism of N_2 fixation. The expression of heterologous nitrogenase enables the engineered *S. elongatus* PCC 7942 strain to perform the N_2 fixation constantly. In the e-BNF system, methyl viologen (MV) serves as the electron mediator to supply enough external electrons from the cathode for the turnover of nitrogenase. Depending on the external electron supply, the engineered *S. elongatus* PCC 7942

cells are employed to perform N_2 fixation in the e-BNF system under illumination. Finally, the secreted extracellular NH_3 is characterized and quantified.

RESULTS AND DISCUSSION

Design of the *nif* gene cluster

There are three known types of nitrogenase, in which the central component of their catalytic protein metalloclusters are molybdenum (Mo), vanadium (V), and iron (Fe)[44]. The Mo-dependent nitrogenase, which is the most common nitrogenase in diazotrophs, is a complex oxidoreductase enzymatic system consisting of two metalloproteins: dinitrogenase (iron-molybdenum protein [MoFe protein]) and dinitrogenase reductase (iron-protein [FeP]).[11] As shown in Figure 1B, a minimal *nif* gene cluster from *Paenibacillus* sp. WLY78.7 (GenBank: ALJV00000000.1),[27] supplemented with genes to express protein NifU (GenBank: WP_004138782.1), NifS (GenBank: WP_024360010.1), NifQ (GenBank: WP_025107738.1), and NifZ (GenBank: WP_004138777.1), was integrated into the genome of *S. elongatus* PCC 7942 for the heterologous expression of nitrogenase. The MoFe protein consists of two different peptide chains encoded by *nifD* and *nifK*, which are associated as a mixed ($\alpha_2\beta_2$) tetramer containing a P-cluster [Fe_8S_7] and FeMo-co [(*R*-homocitrate) Mo-Fe_7S_9C] cluster, in which dinitrogen molecules are reduced stepwise to ammonia. The FeP is a homodimer (encoded by *nifH*) bridged by an intersubunit [4Fe-4S] cluster, which serves as the electron donor to the MoFe protein.[41] Apart from the structural genes *nifK*, *nifD*, and *nifH*, a number of additional genes are also required for the synthesis and insertion of metalloclusters into nitrogenase. Some previous research indicated that NifB, NifE, NifN, and NifH proteins had important roles in the synthesis and assembly of FeMo-co cofactor in the presence of Fe^{2+}, S^{2-}, MoO_4^{2-}, and homocitrate.[45] Accordingly, a *nif* gen cluster with six conserved genes *nifH*, *nifD*, *nifK*, *nifE*, *nifN*, and *nifB* was designed. Seven additional genes, including *nifS*, *nifU*, *nifX*, *nifV*, *nifQ*, *nifZ*, and *hesA*, were also included in the *nif* gene cluster to act in a chaperone-like manner for metalloclusters assembly and insertion.[46,47] The protein scaffolds NifS and NifU mobilize Fe and S for the synthesis of [Fe_4S_4] clusters. Here, NifV is responsible for synthesizing the homocitrate moiety of FeMo-co,[48] NifQ serves as a Mo transporter, and NifB, NifEN, and NifX have critical roles in FeMo-co maturation and its transfer to NifDK proteins.[49] NifZ acts as a chaperone that facilitates the P-cluster maturation for the MoFe protein.[50] The role of the *hesA* gene in the *nif* gene cluster of *Paenibacillus* sp. WLY78.7 is unclear, but it was expected to be related to the introduction of S and Mo for diazotrophic cyanobacteria.[27,51]

The *nif* gene cluster is a long one, approximately 15 kb. If the entire *nif* gene cluster is under the control of a single promoter, the length of the resultant, long, polycistronic mRNA would be restricted by the capability of the RNA polymerase and would result in expression levels of genes in decreasing order.[52] To address that issue, the entire *nif* gene cluster was divided into six segments, and every segment had an independent promoter and terminator. As a result, mRNA transcripts of each gene segment can be generated independently of the entire read-through transcript.

The expression of nitrogenase subunits (NifD, NifK, and NifH protein) was verified by western blot. Because no tag was fused with any subunit of the nitrogenase, to protect the activity of the nitrogenase, the polyclonal antibodies (anti-NifD, anti-NifK, and anti-NifH antibody) were designed and prepared by GenScript. As shown in Figure S1, the cell lysis of the engineered *S. elongatus* PCC 7942 strain with pAM2991-*nif* plasmid (*Se-nif* strain) has the corresponding immunoblotting bands of NifD,

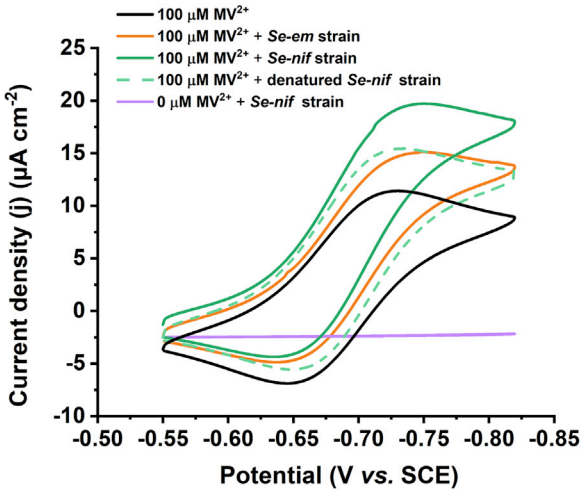

Figure 2. Representative cyclic voltammograms of intracellular nitrogenase turnover mediated by MV

Black line: the current response of 100 μM MV background. Scan rate: 5 mV/s; orange line: the current response of 100 μM MV solution (100 mM MOPS, pH = 7.0, 6.7 mM $MgCl_2$), supplemented with the *Se-em* strain (final OD_{730} = 2). Scan rate: 5 mV/s; green line: the current response of 100 μM MV solution supplemented with the *Se-nif* strain (final OD_{730} = 2). Scan rate: 5 mV/s; green dash line: the current response of 100 μM MV solution supplemented with the *Se-nif* strain harboring the denatured nitrogenase (final OD_{730} = 2). Scan rate: 5 mV/s; purple line: the current response of 0 μM MV and supplemented with the *Se-nif* strain (final OD_{730} = 2). Scan rate: 5 mV/s.

NifK, and NifH on western blot. The cell lysis of the engineered *S. elongatus* PCC 7942 strain with an empty pAM2991 plasmid (*Se-em* strain) did not exhibit any immunoblotting band on the western blot at the same location. In addition to western blot, reverse transcription PCR (RT-PCR) was employed to further detect the transcription of every single gene of the *nif* gene cluster. The RT-PCR analysis of the RNA sample isolated from *Se-nif* strain indicated that all of the genes that make up the *nif* gene cluster had been transcribed (Figure S2A). However, the RT-PCR analysis of the RNA samples isolated from the *Se-em* strain did not exhibit any transcription signal of the *nif* gene cluster (Figure S2B). Combining the results of western blot and RT-PCR, the transcription and expression of intracellular nitrogenase in the *Se-nif* strain could be confirmed.

Use of MV as an electron mediator

To avoid the interference of the intracellular redox balance of the engineered strain caused by N_2 reduction and to guarantee sufficient electron supply for the turnover of nitrogenase, MV was employed as an electron mediator to supply external electrons for the turnover of intracellular nitrogenase. MV is a suitable small-electron shuttle, which has been proven to drive the turnover of nitrogenase.[2] Moreover, in some previous studies, MV has been shown to penetrate the cell wall and membrane and finally to permeate into the intracellular environment of *Synechocystis* sp. PCC 6803 and *S. elongatus* PCC 7942 cell.[53–55] Cyclic voltammetry (CV) was used to demonstrate that MV was able to act as the electron mediator to shuttle electrons into the *S. elongatus* PCC 7942 cell and to support the turnover of intracellular nitrogenase. As shown in Figure 2, the CV of 100 μM MV indicated the oxidized MV^{2+} was reduced to $MV^{+\cdot}$ at approximately −0.72V versus a saturated calomel electrode (SCE). Upon the addition of the *Se-em* strain, a current response was observed, showing that the *Se-em* strain was able to communicate with the electrode via the MV mediator. The background metabolic activity of the *Se-em* strain is expected

to consume the external electrons and cause the current response. Once the *Se-nif* strain was introduced, a more obvious catalytic current response at −0.72V versus the SCE was observed. The only difference between *Se-nif* and *Se-em* strain was the heterologously expressed nitrogenase (Figures S1 and S2). Consequently, it was expected that the reduced MV cation radical ($MV^{+\cdot}$), generated from the cathode-delivered external electrons into the *Se-nif* cell, supported the proton reduction catalyzed by the intracellular nitrogenase and, finally, caused the higher current response. To further verify that speculation, the intracellular nitrogenase of *Se-nif* strain was deactivated by exposure to oxygen bubbling for 2 h. After the intracellular nitrogenase was deactivated, the only difference between the *Se-nif* and *Se-em* strain was eliminated. As expected, the current response dropped to the same level as that of the *Se-em* strain. This result once again confirmed the difference in current response between *Se-nif* and *Se-em* strain was caused by the turnover of the intracellular nitrogenase. To maintain the high electron flow for the future bioelectrocatalytic nitrogen fixation, the working potential of the e-BNF system was determined to be −0.85 V versus that of the SCE.

Intracellular nitrogenase activity assay and optimization

An inherent challenge of using the engineered *Se-nif* strain to heterologously express nitrogenase is the trade-off between O_2 and ATP generation. On one side, the O_2 generated via photosynthetic water splitting catalyzed by photosystem II (PSII) deactivated the expressed O_2-sensitive nitrogenase. Meanwhile, O_2 is indispensable for cell respiration and the efficient generation of ATP. Because the expression of a recombinant protein is an energy-consuming process,[56] the excessive suppression of O_2 production is not conducive to the effective expression of nitrogenase. Therefore, it is crucial to regulate the generation rate of O_2 and to keep the intracellular O_2 concentration at an appropriate level during the nitrogenase-induction stage. In this study, a commonly used PSII inhibitor, 3-(3,4-dichlorophenyl)-1,1-dimethylurea (DCMU), was employed during the nitrogenase-induction stage to regulate the O_2 generation rate. DCMU blocks the plastoquinone binding site of PSII, inhibiting the PSII function and the ability to generate O_2 when illuminated.[57] In the stage of intracellular nitrogenase activity assay and NH_3 production, DCMU was no longer added to the reaction system to avoid the interference of photosynthesis. The reduced $MV^{+\bullet}$ generated from the cathode can permeate into the cell and convert the generated O_2 to reactive oxygen species (ROS), including H_2O_2, superoxide, and hydroxyl radical.[55] The generated ROS would be further scavenged by the ROS-scavenging system of the cyanobacteria, which includes ROS-scavenging enzymes (superoxide dismutase and catalase) and antioxidants (carotenoid and tocopherols).[58]

As shown in Figure 3A, the *Se-nif* strain exhibited different intracellular nitrogenase activity after induction with 1 mM isopropyl thiogalactoside (IPTG) and DCMU at different concentrations. The *Se-nif* strain without the addition of DCMU exhibits no acetylene (C_2H_2) reduction activity because of the nitrogenase deactivation caused by intracellular O_2. Upon addition of 50 μM DCMU, the *Se-nif* strain exhibited the greatest C_2H_2 reduction activity (342 nmol optical density 730 $[OD_{730}]^{-1}$ L^{-1} h^{-1}), indicating 50 μM was the best concentration of DCMU. The continuous increase of the DCMU concentration to 500 μM decreased the C_2H_2-reduction activity of the *Se-nif* strain. This result was expected to be caused by excessively suppressed photolysis of water and the generation of O_2. The insufficient O_2 generation was also unconducive to the smooth progress of cell respiration and ATP generation and finally suppressed the expression of nitrogenase. Furthermore, excessive inhibition of PSII also decreases the efficiency of the photosynthetic phosphorylation and ATP

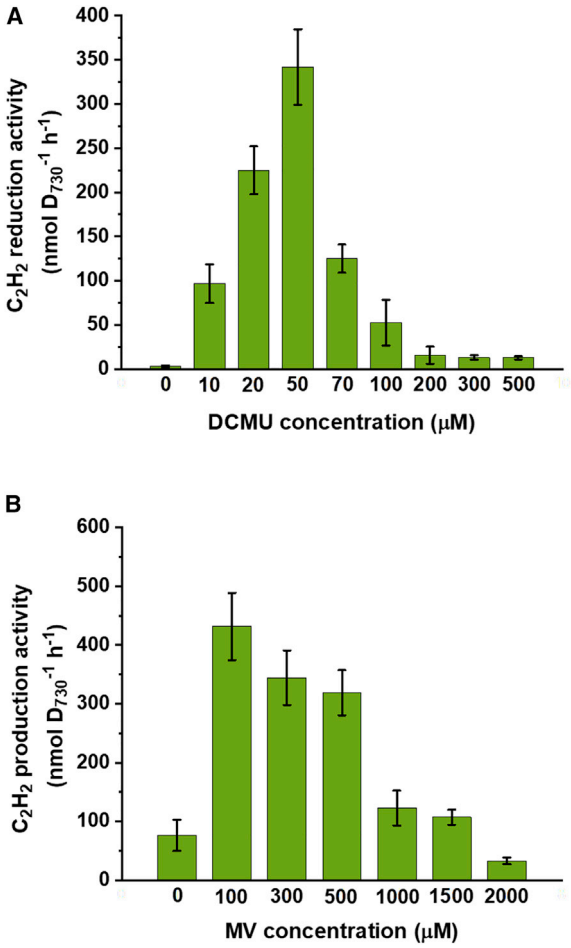

Figure 3. Nitrogenase activity assay and optimization

(A and B) The nitrogenase activity of *Se-nif* strain at different concentrations of DCMU (A). The nitrogenase activity of *Se-nif* strain at different concentrations of MV (B). The nitrogenase activity assays were performed in 3 mL sterilized and degassed MOPS buffer (100 mM, pH = 7.0) supplemented with 6.7 mM $MgCl_2$. The final cell density of the *Se-em* strain was set at OD_{730} = 2. The error bars on the C_2H_2 reduction activity are the standard deviations of the average values.

generation. The final optimized concentration of DCMU was determined to be 50 μM. As shown in Figure 3B, the concentration of MV has an evident effect on the nitrogenase activity of the *Se-nif* strain as well. In the absence of MV, the turnover of intracellular nitrogenase only depended on the endogenous electron supply of the *Se-nif* strain. Accordingly, the *Se-nif* strain only exhibited 76 nmol OD_{730}^{-1} L^{-1} h^{-1} reduction activity. Upon addition of 100 μM MV, the C_2H_2 reduction activity increased approximately 5.7 times to 431 nmol OD_{730}^{-1} L^{-1} h^{-1}. This significant improvement in C_2H_2 reduction activity indicated the advantage of the external electron supply toward the turnover of intracellular nitrogenase. The reduced $MV^{+\cdot}$ transported sufficient electrons into the *Se-nif* strain and eliminated the dependence of nitrogenase on the endogenous electron supply, and finally, improved the turnover of the nitrogenase. Continuously increasing the concentration of MV to 2,500 μM caused a gradual decrease in the C_2H_2-reduction activity, which was probably caused by the toxicity of the electron mediator to the cell or enzyme in high concentrations.[59,60] Herein, the toxicity of MV is an unavoidable problem. We first evaluated the effect of MV concentration on cell growth

(Figure S3). After working in the e-BNF system for 48 h, the final cell density of the *Se-nif* strain did not exhibit an obvious difference under different concentrations of MV from 0 to 500 μM, which indicated that the cells had adapted to the increase in the mediator within that range. It is highly possible that the toxicity of the MV does not come from the mediator itself but from the sudden shift in the reducing balance inside the bacteria. According to previous studies, the addition of reduced mediators changed the intracellular NAD/NADH ratio by replacing ferredoxin in the redox reactions catalyzed by enzymes involved in the distribution of the electron flow.[61,62] Therefore, this gradual decrease in the C_2H_2-reduction activity at a high MV concentration was probably caused by the shift in the intracellular reducing balance based on the continuous reducing power input. The shift in reducing balance may further change the transmembrane electrochemical gradient of the mitochondria and the thylakoid. Finally, it adversely affected the production of ATP. In addition, the dark-blue color of the reduced $MV^{+\cdot}$ at a high concentration hindered the effective transmission of light and, ultimately, reduced the efficiency of the photosynthetic phosphorylation and ATP generation. For the *Se-em* strain, the C_2H_2-reduction activity was not detectable under any concentration of DCMU and MV because no intracellular nitrogenase was expressed. Accordingly, 100 μM of mediator MV was employed in the following bioelectrocatalytic N_2 fixation.

Bioelectrocatalytic synthesis of NH_3

To achieve high NH_3 production, the cell density of the *Se-nif* strain was also optimized. In the practical N_2 fixation process, the high cell density was equivalent to high nitrogenase loading. As shown in Figure 4A, the NH_3 concentration could be increased from 14 μM to 84 μM after 7 h of reaction with an increase in the cell density from OD_{730} = 0.5 to 6. Meantime, the *Se-em* strain also produced an NH_3 accumulation, which was expected to be generated from the background metabolic activity of the host cell (i.e., the transamination and deamination catalyzed by intracellular enzymes). To further distinguish the NH_3 generated from background cellular metabolic activities and the turnover of intracellular nitrogenase, proton nuclear magnetic resonance spectroscopy (^{1}H NMR) was further employed to detect $^{15}NH_4^+$ produced from the reduction of $^{15}N_2$ catalyzed by nitrogenase because it can directly distinguish $^{15}NH_4^+$ from $^{14}NH_4^+$. The scalar interaction between ^{1}H and ^{15}N in $^{15}NH_4^+$ induces the ^{1}H resonance split into a doublet with a spacing of 75 Hz, whereas the ^{1}H resonance coupled to ^{14}N in $^{14}NH_4^+$ is divided into three symmetric signals with a spacing of 52 Hz (Figure S4). As shown in Figure 4B, obvious diagnostic peaks of $^{15}NH_4^+$, which were generated from the reduction of $^{15}N_2$ catalyzed by the intracellular nitrogenase of the *Se-nif* strain, were observed after 7 h of reaction. H–N decoupling proved those protons to be coupled to ^{15}N. Under the same conditions, the *Se-em* strain and the *Se-nif* strain with denatured nitrogenase after 2 h of O_2 bubbling did not exhibit any ^{15}N coupling of the $^{15}NH_4^+$. This result indicated that the NH_3 accumulation of the *Se-em* strain was only generated from the background cellular metabolic activities. In contrast, the NH_3 accumulation of the *Se-nif* strain was caused by both cellular metabolic activity and nitrogenase turnover.

To investigate the NH_3 accumulation generated from nitrogenase turnover following a time course, quantitative NMR was further employed to determine the ratio of $^{15}NH_4^+$ and $^{14}NH_4^+$ during the reduction of $^{15}N_2$ catalyzed by intracellular nitrogenase. As shown in Figures 5A and 5B, the ratio of $^{15}NH_4^+$ to $^{14}NH_4^+$ increased from 25% to 103% throughout 20 h of reaction. Extending the reaction time to 48 h, the ratio of $^{15}NH_4^+$ to $^{14}NH_4^+$ decreased to 38%. The tracking measurement of cell density (Figure S5B) shows that cell density had been slightly reduced after

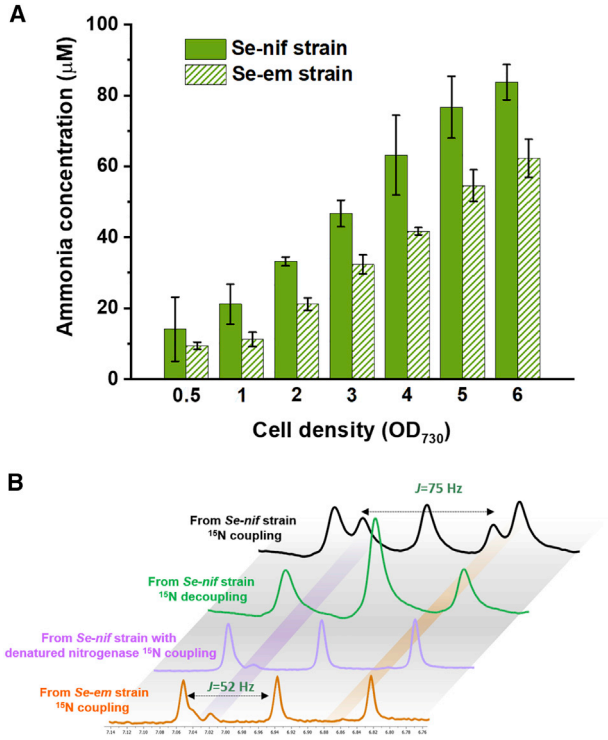

Figure 4. NH_3 accumulation and ^1H NMR spectroscopic determination of $^{15}NH_3$ production

(A) The NH_3 accumulation concentration of *Se-nif* and *Se-em* strains at different cell densities after 7 h of reaction. The reactions were performed in 3 mL sterilized and degassed MOPS buffer (100 mM, pH = 7.0) supplemented with 100 μM MV and 6.7 mM $MgCl_2$. The error bars on the ammonia concentration are the standard deviations of the average values.

(B) ^1H NMR spectroscopic determination of $^{15}NH_3$ produced via the reduction of $^{15}N_2$ catalyzed by *Se-nif* (black and green), denatured *Se-nif* strain (purple), and the *Se-em* strain (orange) at −0.85 V versus SCEs for 7 h. The cell density was set at OD_{730} = 6.

20 h of reaction. The lysis of cells probably caused the release of intracellular $^{14}NH_4^+$ and the decline of the ratio of the $^{15}NH_4^+$ to $^{14}NH_4^+$ in the electrolyte. According to the total accumulation concentration of NH_3 (Figure S5A), the NH_3 accumulation concentration generated from the nitrogenase turnover (the concentration of $^{15}NH_4^+$) after the time course was calculated. As shown in Figure 5C, the concentration of $^{15}NH_4^+$ increased from 15.5 μM to 108 μM through 20 h of reaction. Although the ratio of $^{15}NH_4^+$ to $^{14}NH_4^+$ exhibited a downward trend from 20 h to 48 h, the $^{15}NH_4^+$ concentration further increased to 173 μM because of the continuous turnover of intracellular nitrogenase. The volumetric ammonium evolution rate in 48 h was 3.6 μM/h. The faradaic efficiency (FE) (Figure 5D) of $^{15}NH_4^+$ generation exhibited an upward trend in the first 20 h of the run and achieved the highest level (8.54%) at 20 h. After extending the run time to 48 h, the faradaic efficiency slightly decreased to approximately 6.85%. To further verify the effect of external electron supply mediated by MV on NH_3 production, the $^{15}NH_4^+$ generated from *Se-nif* with and without MV at open circuit conditions was analyzed as well (Figure S6). The result, once again, confirms the promotion effect of the external electron supply on NH_3 production. After 48 h of reaction, the $^{15}NH_4^+$ generated from *Se-nif* without MV as electron mediator was only 8.2 μM. Consequently, the $^{15}NH_4^+$ produced by the *Se-nif* strain with the external electron supply was approximately 21 times greater than that of *Se-nif* without MV after 48 h of reaction. Although the e-BNF system consumed electrical energy, the N_2 fixation efficiency was dramatically

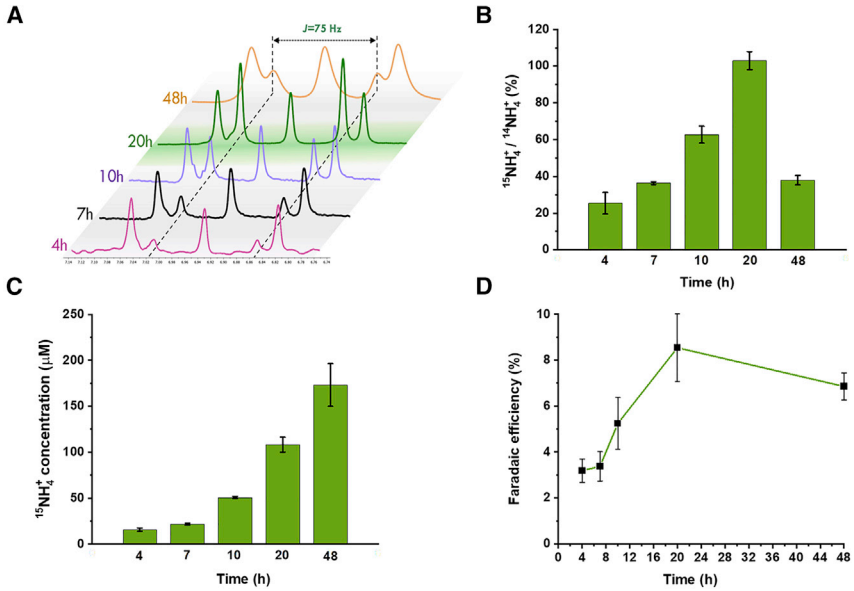

Figure 5. $^{15}NH_4^+$ production and faradaic efficiency following a time course

(A) ^{1}H NMR spectroscopic determination of $^{15}NH_3$ produced by the reduction of $^{15}N_2$ catalyzed by *Se-nif* following a time course.

(B) The ratio of $^{15}NH_4^+$ to $^{14}NH_4^+$ following a time course. The error bars on the ratio of $^{15}NH_4^+$ to $^{14}NH_4^+$ are the standard deviations of the average values.

(C) The calculated concentration of the $^{15}NH_4^+$ produced via nitrogenase turnover. The error bars on the calculated concentration of $^{15}NH_4^+$ produced are the standard deviations of the average values.

(D) The faradaic efficiency of $^{15}NH_4^+$ production following a time course. The NH_3 accumulation was performed in 3 mL sterilized and degassed MOPS buffer (100 mM, pH = 7.0), supplemented with 100 μM MV and 6.7 mM $MgCl_2$ at −0.85 V versus SCEs.

The cell density was set at OD_{730} = 6. The error bars on the faradaic efficiency of $^{15}NH_4^+$ production are the standard deviations of the average values.

increased compared with that driven solely by photosynthesis. In this study, the greatest faradaic efficiency achieved 8.54% after 20 h of reaction. It is conceivable that if a more direct and effective electron transfer pathway between the cathode and the intracellular nitrogenase could be established in the future, the energy efficiency and the NH_3 production efficiency of the e-BNF system could be obviously improved. In that case, the generated NH_3 with a relatively high concentration could be used as a biofertilizer, even as a feedback of the amine chemicals.[63]

In some previous studies related to the e-BNF system, the promoting effect of an external electron supply on microbial N_2 fixation has also been proven. In the Rago et al.[64] study, the biomass synthesis of the autotrophic nitrogen-fixing microorganisms on the electroactive biofilm at electrostimulation conditions was 18 times greater than that in the open-circuit condition. With an external electron supply of 200 μg/L • d N fixation, an assimilation rate was achieved. In another study,[21] the living cells of *Xanthobacter autotrophicus*, which simultaneously express hydrogenase and nitrogenase, were used in the electrochemical water splitting, supporting the e-BNF system in performing N_2 fixation. Based on the external electron supply, the accumulated concentration of extracellular NH_3 in media achieved 11 mg/L (~0.8 mM) after 5 days of reaction. The NMR was only used to qualitatively analyze the generation of $^{15}NH_4^+$.[21] In our research, the accurate concentration of extracellular $^{15}NH_4^+$ was further analyzed via quantitative NMR to evaluate the effectiveness of the microbial e-BNF system.

In this study, the non-diazotrophic cyanobacteria *S. elongatus* PCC 7942 was engineered for N_2 fixation via the introduction of a modified heterologous *nif* gene cluster and heterologous expression of nitrogenase from *Paenibacillus* sp. WLY78.7. The engineered strain of *S. elongatus* PCC 7942 obtained was used to heterologously express nitrogenase via the addition of IPTG and DCMU and further employed in an e-BNF to perform N_2 reduction and NH_3 generation with MV as an electron mediator. The e-BNF system supplied adequate external electrons to significantly improve the turnover of the intracellular nitrogenase. Ultimately, microbial N_2 reduction and NH_3 production were successfully achieved and quantified. The e-BNF system of this study provides novel technological feasibility for the synthesis of NH_3 powered by electrical energy.

EXPERIMENTAL PROCEDURES

Resource availability

Lead contact

Further information and requests for resources and materials should be directed to, and will be fulfilled by, the lead contact, H.C. (chen.hui@utah.edu).

Materials availability

All of the unique materials generated in this study are available from the lead contact upon reasonable request.

Data and code availability

All data associated with the study are included in the article and the Supplemental information. Additional information is available from the lead contact upon reasonable request.

Materials and chemicals

Unless specified otherwise, all chemicals were purchased from Sigma-Aldrich. IPTG was purchased from GoldBio. AvCarb paper was purchased from the Fuel Cell Store (lot no. 190-1419). GCEs (area 0.071 cm^2) and SCEs were obtained from CH Instruments. The cyanobacteria cloning vector pAM2991 was purchased from Addgene. The *nif* gene cluster was synthesized and cloned into the pAM2991 plasmid by GenScript. The primary antibodies, including anti-NifD, anti-NifK, and anti-NifH antibodies (polyclonal antibodies), were designed and synthesized by GenScript. The secondary antibody (mouse anti-rabbit immunoglobulin G [IgG] fragment crystallizable region [Fc] antibody [horseradish peroxidase (HRP)]) for western blot was also purchased from GenScript. The *Synechococcus elongatus* PCC7942 was purchased from American Type Culture Collection (ATCC 33912).

Plasmid transformation

The transformation of the *S. elongatus* PCC 7942 strain was performed by incubating cells at the mid-log phase (OD_{730} of 0.4–0.6) with 200 ng plasmid DNA overnight in the dark. The culture was then spread on a BG-11 agar plate (BG-11 medium, Sigma-Aldrich, 73816; 1.5% [w/v] agar) with 10 mg/mL spectinomycin. The plates were incubated under 150 μE/s/m^2 light condition at 30°C for approximately 2 weeks.

Culture of *S. elongatus* PCC 7942 and nitrogenase induction

The *S. elongatus* PCC 7942 strains, including the wild type and the engineered strains *Se-em* and *Se-nif*, were cultured in BG-11 medium containing 50 mM $NaHCO_3$ under 150 μE/s/m^2 light condition at 30°C and 200-rpm shaking. Cell growth was monitored by measuring OD_{730} with a Beckman Coulter DU-800 spectrophotometer. For nitrogenase induction, precultured cells were collected at

OD_{730} = 0.6, then, transferred into an anaerobic glove bag. The collected cells were washed with degassed, fresh BG11 medium and resuspended in degassed, fresh BG11 medium containing 50 mM $NaHCO_3$, 50 μM $FeCl_3$, and 50 μM Na_2MoO_4. Finally, 1 mM (final concentration) IPTG was added to induce the expression of nitrogenase. To protect the O_2-sensitive nitrogenase, DCMU at different concentrations was added to inhibit the activity of PSII and the generation of oxygen. The cells were cultured and induced in anaerobically sealed vials for 48 h under 150 μE/s/m^2 illumination at 30°C for future use.

Nitrogenase activity assay

Nitrogenase activity was determined with an acetylene-reduction assay. The assay was operated within custom-made, septum-sealed, H-shaped electrochemical cells, where a Nafion 212 proton-exchange membrane was used to compartmentalize the anodic and cathodic chambers. AvCarb carbon paper electrodes were cut and coated with paraffin wax to regulate their geometric surface area and to prevent corrosion upon contact with their electrical contacts. The working electrode area was 1 cm^2. Platinum mesh was used as a counter electrode, and SCE were used as reference electrodes for all the electrochemical experiments. A CH Instruments Electrochemical Work Station was used for the electrochemical measurements. The *S. elongatus* PCC 7942 cells were collected by centrifugation, washed three times, and then resuspended with 3 mL sterilized and degassed MOPS (3-(*N*-morpholino)propanesulfonic acid) buffer (100 mM, pH = 7.0) with 6.7 mM $MgCl_2$ to a final OD_{730} = 2 after induction. MV^{2+} at different concentrations was used as an electron mediator. The head space of the H-shaped electrochemical cells was filled with an atmosphere of 0.1 atm C_2H_2 and 0.9 atm Ar. The working potential was set at −0.85 V versus the SCEs. The reaction was performed under 150 μE/s/m^2 light conditions. The reductive product of C_2H_2 (C_2H_4) was quantified by gas chromatography-flame ionization detection (GC-FID; HP PLOT Q column, using He as the carrier gas).

Cyclic voltammetric analysis

The initial cyclic voltammetric analysis was used to demonstrate the ability of the cathode to act as the primary electron donor for the N_2 reduction catalyzed by the intracellular nitrogenase, in which MV^{2+} served as an electron mediator between the electrode and nitrogenase. To obtain an obvious current response, the *S. elongatus* PCC 7942 cells were immobilized on the surface of electrode, and 10 mL of cell culture was collected after 48 h of induction with a final OD_{730} of ~2.0. The sample was centrifuged at 5,000 rpm for 20 min to collect the cell pellet. The cell pellet was washed with 10 mL degassed MOPS buffer (100 mM, pH = 7.0) in a glove bag. The sample was centrifuged again to collect the cells. The cells were resuspended with 10 μL degassed MOPS buffer (100 mM, pH = 7.0) in the glove bag. The cells suspension was then mixed with 10 μL of sodium alginate solution (3%, w/v), and 10 μL of the resultant mixture was drop-casted onto the AvCarb paper electrode. Then, the electrode was dipped in a calcium chloride solution (2%, w/v) to form an alginate hydrogel coating on the electrode. The resultant electrode was dried in vacuum for 30 min.

A CH Instruments Electrochemical Work Station was used for all electrochemical measurements. A platinum counter electrode, an SCE reference, and a glass-carbon working electrode were used in a three-electrode system. CV was conducted in a sealed three-neck, round-bottom flask and was performed with 100 μM MV^{2+} and 6.7 mM $MgCl_2$ in the anaerobic glove bag. The electrodes were allowed to stabilize

by scanning the potential between −0.82 and −0.55 V versus the SCEs for eight cycles with a scan rate of 5 mV/s.

Bioelectrocatalytic N_2 fixation

For the bioelectrocatalytic N_2 fixation, the culture of the *S. elongatus* PCC 7942 was collected by centrifugation, washed three times, and then, resuspended to a final OD_{730} of 2.5 with 3 mL sterilized and degassed MOPS buffer (100 mM, pH = 7.0) containing 6 mM $MgCl_2$. MV^{2+} was used as the electron mediator. The headspace of the H-shaped electrochemical cell was filled with 1 atm high-purity nitrogen gas (N_2 or $^{15}N_2$). The constant potential applied was selected as −0.85 V versus the SCEs to ensure sufficient overpotential to drive the reaction into the reduction of MV^{2+}. 2 mM *L*-methionine sulfoximine (Sigma-Aldrich, M5379) was added as an irreversible glutamine synthetase inhibitor to inhibit the ammonia assimilation.[65] The N_2 fixation was performed under 150 μE/s/m^2 light condition. The electrolyte was withdrawn at different time points and then centrifuged with a 3 kDa Amicon ultra-centrifugal filter (Sigma-Aldrich, USA) to collect the supernatant. The concentration of the generated ammonia in the supernatant was determined by using an ammonia assay kit (Sigma-Aldrich) following the user's manual.

In vivo $^{15}N_2$ assimilation assay

The reduction of $^{15}N_2$ was used to confirm the production of the NH_3 by intracellular nitrogenase. The headspace of the H-shaped electrochemical cell was filled with 1 atm high-purity $^{15}N_2$ (Cambridge Isotope Laboratories). The electrolyte was withdrawn at the due reaction time and, then, centrifuged to collect the supernatant. The supernatant was spun through a 3 kDa molecular weight cutoff (MWCO) membrane to remove the proteins. HCl was added to a final concentration ~0.1 M to protonate $^{15}NH_3$ for NMR spectroscopy. ^1H ($\pm^{15}N$ decoupling) experiments were used to confirm the identity of $^{15}NH_4^+$. The accurate molar ratio of $^{15}NH_4^+$ to $^{14}NH_4^+$ was measured by relative-concentration quantification NMR. The molar ratio $M(^{15}NH_4^+)/M(^{14}NH_4^+)$ can be determined using the following formula:

$$\frac{M\left(^{15}NH_4^+\right)}{M\left(^{14}NH_4^+\right)} = \frac{I\left(^{15}NH_4^+\right)}{I\left(^{14}NH_4^+\right)} \times \frac{N\left(^{14}NH_4^+\right)}{N\left(^{15}NH_4^+\right)}$$

Here I is the integral, and N is the number of nuclei giving rise to the signal (here, N = 1).[66] Data presented are mean values determined based on results from at least three replicate cultures.

The faradaic efficiency (FE) for the formation of $^{15}NH_4^+$ was calculated as follows:

$$FE = \frac{Fn}{\int_0^t Idt} \times 100\%$$

where F is the faraday constant (96,485 C/mol), n is the moles of generated $^{15}NH_4^+$ (herein, n = 4 because the generation of 1 mol $^{15}NH_4^+$ consumed 4 mol electrons), I is the circuit current, and t is the reaction time.

Western blot analysis

The protein samples analyzed were the soluble fractions in the crude extract from the cell lysate of the engineered *Se-em* and *Se-nif* strains. Proteins extraction and western blot analysis was performed via a modified protocol based on a previous study.[67] In detail, 5 mL of culture was harvested from an OD_{730} = 2 culture by centrifugation at 4,500 rpm, 4°C, for 5 min. The pellet was washed in 2 mL PBS buffer and collected again by centrifugation at 4,500 rpm, 4°C, for 5 min. Then, 200 μL PBS buffer, supplemented with 4 μL of 50 × Protease Arrest (G-Biosciences), was used to resuspend

the pellet, and this mixture was frozen in liquid nitrogen for 4 min, followed by heating at 37°C for 4 min. This process was repeated three times. For the remainder of the procedure, the samples were kept on ice. Acid-washed glass beads (425–600 mm diameter, Sigma-Aldrich) were mixed with the thawed cells. The cells were disrupted by vertexing for 30 s and then resting on ice for 2 min, a process repeated four times. The lysates were collected by centrifuge at 15,000 rpm, 4°C, for 30 s, to get a supernatant containing the soluble proteins.

Total soluble proteins (20 μg) from each strain were loaded into each lane and separated by running through SDS-PAGE gel, using Mini-PROTEAN TGX gels (Bio-Rad) and were transferred to a Trans-Blot Turbo Transfer Pack membrane (Bio-Rad) by a membrane transfer machine (Bio-Rad). Anti-NifH, anti-NifD, and anti-NifK antibodies (polyclonal antibody) were designed and synthesized by GenScript and used to detect the corresponding protein through standard immunoblotting techniques.

RT-PCR

RT-PCR analysis was performed using RNA samples isolated from IPTG treated *Se-em* and *Se-nif* culture grown in BG11 medium at OD_{730} of around 0.6. Genomic DNA was extracted using GenElute bacterial genomic DNA kits purchased from Sigma. Total RNA was extracted using an RNeasy Mini kit purchased from QIAGEN. Genomic DNA and total RNA were quantified on a NanoDrop 2000 spectrophotometer (Thermo Scientific). The RNA samples were treated with 10 μL of RNase-free DNase I mix (QIAGEN) according to manufacturer's instructions. The absence of genomic DNA contamination was checked by PCR using Takara's PrimeSTAR Max DNA polymerase premix and 2 μL total RNA. For cDNA synthesis, 100 ng of DNase-treated RNA samples were used for reverse transcription using the Luna-Script RT SuperMix Kit according to the manufacturer's instructions. PCR was performed using 1 μL of cDNA as template using Takara's PrimeSTAR Max DNA polymerase premix kit. All primers were designed to be about 20 bp in length with a GC content of around 50% and a melting temperature (Tm) of around 62°C. Primers specific against the *S. elongatus* PCC 7942 genome were checked using the NCBI Primer-BLAST tool. All the amplicons were designed to be around 100 bp to ensure high RT-PCR efficiency. The PCR product was then checked by electrophoresis on 3% agarose gel.

SUPPLEMENTAL INFORMATION

Supplemental information can be found online at https://doi.org/10.1016/j.xcrp.2021.100444.

ACKNOWLEDGMENTS

The authors would like to thank Fulcrum Biosciences for funding this research. The authors would like to thank Dr. Sarah E. Soss and Dr. Peter F. Flynn (Department of Chemistry, University of Utah) for help with ^{1}H NMR analysis.

AUTHOR CONTRIBUTIONS

S.D.M. conceived the project and oversaw and coordinated the research; H.C. oversaw and coordinated the research; H.C. and F.D. designed the experiment and established the cell culture and transformation methods; F.D. performed the CV analysis with the help of M.G.; F.D. performed the nitrogenase activity and ammonia production assays; F.D. performed the NMR analysis with the help of Y.S.L.; F.D. and E.M.G. performed the RT-PCR; H.C. and F.D. performed the western blot;

H.H. contributed to the cell culture and transformation; F.D. and H.C. wrote the manuscript; and H.C., F.D., and S.D.M revised the paper. All authors discussed the results and commented on the manuscript.

DECLARATION OF INTERESTS

The authors declare no competing interests.

Received: December 9, 2020
Revised: April 22, 2021
Accepted: May 5, 2021
Published: May 25, 2021

REFERENCES

1. Minteer, S.D., Christopher, P., and Linic, S. (2018). Recent developments in nitrogen reduction catalysts: A virtual issue. ACS Energy Lett. *4*, 163–166.

2. Milton, R.D., Cai, R., Abdellaoui, S., Leech, D., De Lacey, A.L., Pita, M., and Minteer, S.D. (2017). Bioelectrochemical Haber-Bosch process: an ammonia-producing H_2/N_2 fuel cell. Angew. Chem. Int. Ed. Engl. *56*, 2680–2683.

3. Iwamoto, M., Akiyama, M., Aihara, K., and Deguchi, T. (2017). Ammonia synthesis on wool-like Au, Pt, Pd, Ag, or Cu electrode catalysts in nonthermal atmospheric-pressure plasma of N_2 and H_2. ACS Catal. *7*, 6924–6929.

4. Chalkley, M.J., Del Castillo, T.J., Matson, B.D., and Peters, J.C. (2018). Fe-Mediated Nitrogen Fixation with a metallocene mediator: exploring pK_a effects and demonstrating electrocatalysis. J. Am. Chem. Soc. *140*, 6122–6129.

5. Brown, K.A., Harris, D.F., Wilker, M.B., Rasmussen, A., Khadka, N., Hamby, H., Keable, S., Dukovic, G., Peters, J.W., Seefeldt, L.C., and King, P.W. (2016). Light-driven dinitrogen reduction catalyzed by a CdS:nitrogenase MoFe protein biohybrid. Science *352*, 448–450.

6. Chica, B., Ruzicka, J., Kallas, H., Mulder, D.W., Brown, K.A., Peters, J.W., Seefeldt, L.C., Dukovic, G., and King, P.W. (2020). Defining intermediates of nitrogenase MoFe protein during N_2 reduction under photochemical electron delivery from CdS quantum dots. J. Am. Chem. Soc. *142*, 14324–14330.

7. Foster, S.L., Bakovic, S.I.P., Duda, R.D., Maheshwari, S., Milton, R.D., Minteer, S.D., Janik, M.J., Renner, J.N., and Greenlee, L.F. (2018). Catalysts for nitrogen reduction to ammonia. Nat. Catal. *1*, 490.

8. Cherkasov, N., Ibhadon, A., and Fitzpatrick, P. (2015). A review of the existing and alternative methods for greener nitrogen fixation. Chem. Eng. Process. *90*, 24–33.

9. Lindley, B.M., Appel, A.M., Krogh-Jespersen, K., Mayer, J.M., and Miller, A.J. (2016). Evaluating the thermodynamics of electrocatalytic N_2 reduction in acetonitrile. ACS Energy Lett. *1*, 698–704.

10. Seefeldt, L.C., Hoffman, B.M., Peters, J.W., Raugei, S., Beratan, D.N., Antony, E., and Dean, D.R. (2018). Energy transduction in nitrogenase. Acc. Chem. Res. *51*, 2179–2186.

11. Milton, R.D., and Minteer, S.D. (2017). Enzymatic bioelectrosynthetic ammonia production: recent electrochemistry of nitrogenase, nitrate reductase, and nitrite reductase. ChemPlusChem *82*, 513–521.

12. Lee, Y.S., Ruff, A., Cai, R., Lim, K., Schuhmann, W., and Minteer, S.D. (2020). Electroenzymatic nitrogen fixation using an organic redox polymer-immobilized MoFe protein system. Angew. Chem. *59*, 16511–16516.

13. Milton, R.D., Abdellaoui, S., Khadka, N., Dean, D.R., Leech, D., Seefeldt, L.C., and Minteer, S.D. (2016). Nitrogenase bioelectrocatalysis: heterogeneous ammonia and hydrogen production by MoFe protein. Energy Environ. Sci. *9*, 2550–2554.

14. Milton, R.D., Cai, R., Sahin, S., Abdellaoui, S., Alkotaini, B., Leech, D., and Minteer, S.D. (2017). The in vivo potential-regulated protective protein of nitrogenase in *Azotobacter vinelandii* supports aerobic bioelectrochemical dinitrogen reduction *in vitro*. J. Am. Chem. Soc. *139*, 9044–9052.

15. Patel, J., Cai, R., Milton, R., Chen, H., and Minteer, S.D. (2020). Pyrene-based noncovalent immobilization of nitrogenase on carbon surfaces. ChemBioChem *21*, 1729–1732.

16. Dos Santos, P.C., Fang, Z., Mason, S.W., Setubal, J.C., and Dixon, R. (2012). Distribution of nitrogen fixation and nitrogenase-like sequences amongst microbial genomes. BMC Genomics *13*, 162.

17. Knoche, K.L., Aoyama, E., Hasan, K., and Minteer, S.D. (2017). Role of nitrogenase and ferredoxin in the mechanism of bioelectrocatalytic nitrogen fixation by the cyanobacteria *Anabaena variabilis* SA-1 mutant immobilized on indium tin oxide (ITO) electrodes. Electrochim. Acta *232*, 396–403.

18. Callahan, S.M., and Buikema, W.J. (2001). The role of HetN in maintenance of the heterocyst pattern in *Anabaena* sp. PCC 7120. Mol. Microbiol. *40*, 941–950.

19. Yoch, D.C., and Gotto, J.W. (1982). Effect of light intensity and inhibitors of nitrogen assimilation on NH_4^+ inhibition of nitrogenase activity in *Rhodospirillum rubrum* and *Anabaena* sp. J. Bacteriol. *151*, 800–806.

20. Wolk, C.P. (2000). Heterocyst formation in *Anabaena*. In Prokaryotic Development, Y.V. Brun and L.J. Shimkets, eds. (American Society of Microbiology), pp. 83–104.

21. Liu, C., Sakimoto, K.K., Colón, B.C., Silver, P.A., and Nocera, D.G. (2017). Ambient nitrogen reduction cycle using a hybrid inorganic-biological system. Proc. Natl. Acad. Sci. USA *114*, 6450–6455.

22. Solomon, J.B., Lee, C.C., Jasniewski, A.J., Rasekh, M.F., Ribbe, M.W., and Hu, Y. (2020). Heterologous expression and engineering of the nitrogenase cofactor biosynthesis scaffold NifEN. Angew. Chem. Int. Ed. Engl. *59*, 6887–6893.

23. Xiang, N., Guo, C., Liu, J., Xu, H., Dixon, R., Yang, J., and Wang, Y.-P. (2020). Using synthetic biology to overcome barriers to stable expression of nitrogenase in eukaryotic organelles. Proc. Natl. Acad. Sci. USA *117*, 16537–16545.

24. Burén, S., and Rubio, L.M. (2018). State of the art in eukaryotic nitrogenase engineering. FEMS Microbiol. Lett. *365*, fnx274.

25. Temme, K., Zhao, D., and Voigt, C.A. (2012). Refactoring the nitrogen fixation gene cluster from *Klebsiella oxytoca*. Proc. Natl. Acad. Sci. USA *109*, 7085–7090.

26. Dixon, R.A., and Postgate, J.R. (1972). Genetic transfer of nitrogen fixation from *Klebsiella pneumoniae* to *Escherichia coli*. Nature *237*, 102–103.

27. Wang, L., Zhang, L., Liu, Z., Zhao, D., Liu, X., Zhang, B., Xie, J., Hong, Y., Li, P., Chen, S., et al. (2013). A minimal nitrogen fixation gene cluster from *Paenibacillus* sp. WLY78 enables expression of active nitrogenase in *Escherichia coli*. PLoS Genet. *9*, e1003865.

28. Yang, J., Xie, X., Wang, X., Dixon, R., and Wang, Y.-P. (2014). Reconstruction and minimal gene requirements for the alternative iron-only nitrogenase in *Escherichia coli*. Proc. Natl. Acad. Sci. USA *111*, E3718–E3725.

29. Smanski, M.J., Bhatia, S., Zhao, D., Park, Y., B A Woodruff, L., Giannoukos, G., Ciulla, D., Busby, M., Calderon, J., Nicol, R., et al. (2014). Functional optimization of gene clusters by combinatorial design and assembly. Nat. Biotechnol. *32*, 1241–1249.

30. Liu, D., Liberton, M., Yu, J., Pakrasi, H.B., and Bhattacharyya-Pakrasi, M. (2018). Engineering nitrogen fixation activity in an oxygenic phototroph. MBio *9*, e01029-18.

31. Cheng, Q., Day, A., Dowson-Day, M., Shen, G.-F., and Dixon, R. (2005). The *Klebsiella pneumoniae* nitrogenase Fe protein gene (*nif*H) functionally substitutes for the chlL gene in *Chlamydomonas reinhardtii*. Biochem. Biophys. Res. Commun. *329*, 966–975.

32. Burén, S., Young, E.M., Sweeny, E.A., Lopez-Torrejón, G., Veldhuizen, M., Voigt, C.A., and Rubio, L.M. (2017). Formation of nitrogenase NifDK tetramers in the mitochondria of *Saccharomyces cerevisiae*. ACS Synth. Biol. *6*, 1043–1055.

33. López-Torrejón, G., Jiménez-Vicente, E., Buesa, J.M., Hernandez, J.A., Verma, H.K., and Rubio, L.M. (2016). Expression of a functional oxygen-labile nitrogenase component in the mitochondrial matrix of aerobically grown yeast. Nat. Commun. *7*, 11426.

34. Pérez-González, A., Kniewel, R., Veldhuizen, M., Verma, H.K., Navarro-Rodríguez, M., Rubio, L.M., and Caro, E. (2017). Adaptation of the GoldenBraid modular cloning system and creation of a toolkit for the expression of heterologous proteins in yeast mitochondria. BMC Biotechnol. *17*, 80.

35. Zamir, A., Maina, C.V., Fink, G.R., and Szalay, A.A. (1981). Stable chromosomal integration of the entire nitrogen fixation gene cluster from *Klebsiella pneumoniae* in yeast. Proc. Natl. Acad. Sci. USA *78*, 3496–3500.

36. Burén, S., Pratt, K., Jiang, X., Guo, Y., Jimenez-Vicente, E., Echavarri-Erasun, C., Dean, D.R., Saaem, I., Gordon, D.B., Voigt, C.A., and Rubio, L.M. (2019). Biosynthesis of the nitrogenase active-site cofactor precursor NifB-co in *Saccharomyces cerevisiae*. Proc. Natl. Acad. Sci. USA *116*, 25078–25086.

37. Duval, S., Danyal, K., Shaw, S., Lytle, A.K., Dean, D.R., Hoffman, B.M., Antony, E., and Seefeldt, L.C. (2013). Electron transfer precedes ATP hydrolysis during nitrogenase catalysis. Proc. Natl. Acad. Sci. USA *110*, 16414–16419.

38. Hickey, D.P., Lim, K., Cai, R., Patterson, A.R., Yuan, M., Sahin, S., Abdellaoui, S., and Minteer, S.D. (2018). Pyrene hydrogel for promoting direct bioelectrochemistry: ATP-independent electroenzymatic reduction of N_2. Chem. Sci. (Camb.) *9*, 5172–5177.

39. Lee, Y.S., Yuan, M., Cai, R., Lim, K., and Minteer, S.D. (2020). Nitrogenase bioelectrocatalysis: atp-independent ammonia production using a redox polymer/mofe protein system. ACS Catal. *10*, 6854–6861.

40. Li, X.X., Liu, Q., Liu, X.M., Shi, H.W., and Chen, S.F. (2016). Using synthetic biology to increase nitrogenase activity. Microb. Cell Fact. *15*, 43.

41. Seefeldt, L.C., Peters, J.W., Beratan, D.N., Bothner, B., Minteer, S.D., Raugei, S., and Hoffman, B.M. (2018). Control of electron transfer in nitrogenase. Curr. Opin. Chem. Biol. *47*, 54–59.

42. Wang, B., Xiao, K., Jiang, Z., Wang, J., Jimmy, C.Y., and Wong, P.K. (2019). Biohybrid photoheterotrophic metabolism for significant enhancement of biological nitrogen fixation in pure microbial cultures. Energy Environ. Sci. *12*, 2185–2191.

43. Allen, R.S., Tilbrook, K., Warden, A.C., Campbell, P.C., Rolland, V., Singh, S.P., and Wood, C.C. (2017). Expression of 16 nitrogenase proteins within the plant mitochondrial matrix. Front. Plant Sci. *8*, 287.

44. Zhao, Y., Bian, S.M., Zhou, H.N., and Huang, J.F. (2006). Diversity of nitrogenase systems in diazotrophs. J. Integr. Plant Biol. *48*, 745–755.

45. Curatti, L., Hernandez, J.A., Igarashi, R.Y., Soboh, B., Zhao, D., and Rubio, L.M. (2007). In vitro synthesis of the iron-molybdenum cofactor of nitrogenase from iron, sulfur, molybdenum, and homocitrate using purified proteins. Proc. Natl. Acad. Sci. USA *104*, 17626–17631.

46. Jasniewski, A.J., Lee, C.C., Ribbe, M.W., and Hu, Y. (2020). Reactivity, mechanism, and assembly of the alternative nitrogenases. Chem. Rev. *120*, 5107–5157.

47. Burén, S., Jiménez-Vicente, E., Echavarri-Erasun, C., and Rubio, L.M. (2020). Biosynthesis of nitrogenase cofactors. Chem. Rev. *120*, 4921–4968.

48. Hoover, T.R., Imperial, J., Ludden, P.W., and Shah, V.K. (1988). Homocitrate cures the $NifV^-$ phenotype in *Klebsiella pneumoniae*. J. Bacteriol. *170*, 1978–1979.

49. Hernandez, J.A., Igarashi, R.Y., Soboh, B., Curatti, L., Dean, D.R., Ludden, P.W., and Rubio, L.M. (2007). NifX and NifEN exchange NifB cofactor and the VK-cluster, a newly isolated intermediate of the iron-molybdenum cofactor biosynthetic pathway. Mol. Microbiol. *63*, 177–192.

50. Hu, Y., Fay, A.W., Lee, C.C., and Ribbe, M.W. (2007). P-cluster maturation on nitrogenase MoFe protein. Proc. Natl. Acad. Sci. USA *104*, 10424–10429.

51. Liu, X., Zhao, X., Li, X., and Chen, S. (2019). Suppression of *hesA* mutation on nitrogenase activity in *Paenibacillus polymyxa* WLY78 with the addition of high levels of molybdate or cystine. PeerJ *7*, e6294.

52. Chen, H., Huang, R., and Zhang, Y.P. (2017). Systematic comparison of co-expression of multiple recombinant thermophilic enzymes in *Escherichia coli* BL21(DE3). Appl. Microbiol. Biotechnol. *101*, 4481–4493.

53. Bombelli, P., Bradley, R.W., Scott, A.M., Philips, A.J., McCormick, A.J., Cruz, S.M., Anderson, A., Yunus, K., Bendall, D.S., and Cameron, P.J. (2011). Quantitative analysis of the factors limiting solar power transduction by *Synechocystis* sp. PCC 6803 in biological photovoltaic devices. Energy Environ. Sci. *4*, 4690–4698.

54. Krasikov, V., Aguirre von Wobeser, E., Dekker, H.L., Huisman, J., and Matthijs, H.C. (2012). Time-series resolution of gradual nitrogen starvation and its impact on photosynthesis in the cyanobacterium *Synechocystis* PCC 6803. Physiol. Plant. *145*, 426–439.

55. Tanaka, K., Shimakawa, G., and Nakanishi, S. (2020). Time-of-day-dependent responses of cyanobacterial cellular viability against oxidative stress. Sci. Rep. *10*, 20029.

56. Bai, Z., Harvey, L.M., White, S., and McNeil, B. (2004). Effects of oxidative stress on production of heterologous and native protein, and culture morphology in batch and chemostat cultures of *Aspergillus niger* (B1-D). Enzyme Microb. Technol. *34*, 10–21.

57. Liu, W., Ming, Y., Li, P., and Huang, Z. (2012). Inhibitory effects of hypo-osmotic stress on extracellular carbonic anhydrase and photosynthetic efficiency of green alga *Dunaliella salina* possibly through reactive oxygen species formation. Plant Physiol. Biochem. *54*, 43–48.

58. Takahashi, H., Kusama, Y., Li, X., Takaichi, S., and Nishiyama, Y. (2019). Overexpression of orange carotenoid protein protects the repair of PSII under strong light in *Synechocystis* sp. PCC 6803. Plant Cell Physiol. *60*, 367–375.

59. Xuejiang, W., Dzyadevych, S.V., Chovelon, J.-M., Renault, N.J., Ling, C., Siqing, X., and Jianfu, Z. (2006). Conductometric nitrate biosensor based on methyl viologen/Nafion/nitrate reductase interdigitated electrodes. Talanta *69*, 450–455.

60. Kim, M.-H., and Yun, S.-E. (2004). Construction of an electro-enzymatic bioreactor for the production of (*R*)-mandelate from benzoylformate. Biotechnol. Lett. *26*, 21–26.

61. Peguin, S., Goma, G., Delorme, P., and Soucaille, P. (1994). Metabolic flexibility of *Clostridium acetobutylicum* in response to methyl viologen addition. Appl. Microbiol. Biotechnol. *42*, 611–616.

62. Girbal, L., Vasconcelos, I., Saint-Amans, S., and Soucaille, P. (1995). How neutral red modified carbon and electron flow in *Clostridium acetobutylicum* grown in chemostat culture at neutral pH. FEMS Microbiol. Rev. *16*, 151–162.

63. Chen, H., Cai, R., Patel, J., Dong, F., Chen, H., and Minteer, S.D. (2019). Upgraded bioelectrocatalytic N_2 fixation: from N_2 to chiral amine intermediates. J. Am. Chem. Soc. *141*, 4963–4971.

64. Rago, L., Zecchin, S., Villa, F., Goglio, A., Corsini, A., Cavalca, L., and Schievano, A. (2019). Bioelectrochemical Nitrogen fixation (e-BNF): Electro-stimulation of enriched biofilm communities drives autotrophic nitrogen and carbon fixation. Bioelectrochemistry *125*, 105–115.

65. Ronzio, R.A., Rowe, W.B., and Meister, A. (1969). Studies on the mechanism of inhibition of glutamine synthetase by methionine sulfoximine. Biochemistry *8*, 1066–1075.

66. Malz, F., and Jancke, H. (2005). Validation of quantitative NMR. J. Pharm. Biomed. Anal. *38*, 813–823.

67. Liu, X., Miao, R., Lindberg, P., and Lindblad, P. (2019). Modular engineering for efficient photosynthetic biosynthesis of 1-butanol from CO_2 in cyanobacteria. Energy Environ. Sci. *12*, 2765–2777.